HHS Public Access

Author manuscript

Biomacromolecules. Author manuscript; available in PMC 2018 July 27.

Published in final edited form as:

Biomacromolecules. 2017 October 09; 18(10): 3040–3051. doi:10.1021/acs.biomac.7b00324.

Soft Substrates Containing Hyaluronan Mimic the Effects of Increased Stiffness on Morphology, Motility, and Proliferation of Glioma Cells

Katarzyna Pogoda[†,‡,*], **Robert Bucki**[†,§], **Fitzroy J. Byfield**[†], **Katrina Cruz**[†], **Tongkeun Lee**[†], **Cezary Marcinkiewicz**[‖], and **Paul A. Janmey**[†,⊥]

[†]Institute for Medicine and Engineering, University of Pennsylvania, 3340 Smith Walk, Philadelphia, Pennsylvania 19104, United States [‡]Institute of Nuclear Physics Polish Academy of Sciences, PL-31342 Krakow, Poland [§]Department of Microbiological and Nanobiomedical Engineering, Medical University of Bialystok, 15-222 Bialystok, Poland [‖]CoE Department of Bioengineering, Temple University, Philadelphia, Pennsylvania 19122, United States [⊥]Department of Physiology, University of Pennsylvania, Philadelphia, Pennsylvania 19104, United States

Abstract

Unlike many other cancer cells that grow in tumors characterized by an abnormally stiff collagen-enriched stroma, glioma cells proliferate and migrate in the much softer environment of the brain, which generally lacks the filamentous protein matrix characteristic of breast, liver, colorectal, and other types of cancer. Glial cell-derived tumors and the cells derived from them are highly heterogeneous and variable in their mechanical properties, their response to treatments, and their properties in vitro. Some glioma samples are stiffer than normal brain when measured ex vivo, but even those that are soft in vitro stiffen after deformation by pressure gradients that arise in the tumor environment in vivo. Such mechanical differences can strongly alter the phenotype of cultured glioma cells. Alternatively, chemical signaling might elicit the same phenotype as increased stiffness by activating intracellular messengers common to both initial stimuli. In this study the responses of three different human glioma cell lines to changes in substrate stiffness are compared with their responses on very soft substrates composed of a combination of hyaluronic acid and a specific integrin ligand, either laminin or collagen I. By quantifying cell morphology, stiffness, motility, proliferation, and secretion of the cytokine IL-8, glioma cell responses to increased stiffness are shown to be nearly identically elicited by substrates containing hyaluronic acid, even in the absence of increased stiffness. PI3-kinase activity was required for the response to hyaluronan but not to stiffness. This outcome suggests that hyaluronic acid can trigger the same

[*]Corresponding Author: katarzyna.pogoda@ifj.edu.pl. Tel: +1 267-356-1160.

ORCID

Katarzyna Pogoda: 0000-0001-8405-4564

Author Contributions

K.P. performed most of the cell biology experiments and image analysis. K.P. and F.B. did AFM measurements and analyses. K.C. and T.L. designed and produced the hydrogels and assisted with cell cultures and image analysis. R.B. designed and performed the studies of IL-8 secretion. C.M. provided the LBC3 cells, designed the culture methods for them, and performed preliminary analyses of integrin expression. P.A.J. and K.P. designed the biophysical studies and wrote the manuscript, which was edited by all authors.

Notes

The authors declare no competing financial interest.

cellular response, as can be obtained by mechanical force transduced from a stiff environment, and demonstrates that chemical and mechanical features of the tumor microenvironment can achieve equivalent reactions in cancer cells.

Graphical Abstract

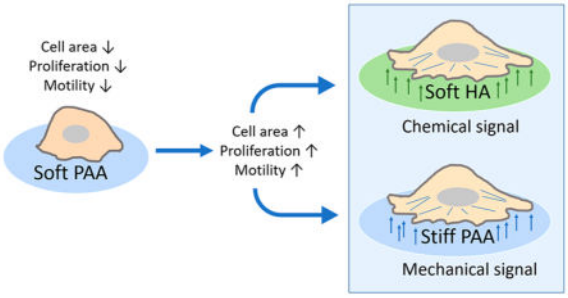

INTRODUCTION

The most common primary malignant glioma, called glioblastoma (GBM), is one of the deadliest cancers among humans. High proliferation rate, invasiveness, and insensitivity to existing treatments result in very poor prognosis and short survival period. GBM tumors are usually highly heterogeneous and consist of regions with different subpopulations of cells and various matrix compositions, which are often associated with treatment failure and development of treatment resistance.[1,2] Glioblastoma cells usually do not create distant metastatic sites in other organs, as is observed for breast, prostate, and liver cancer cells, but rather their migration is limited to the CNS with characteristic rapid infiltration to different brain regions.[3] Brain tissue has a unique composition compared with other soft tissues, like breast or liver. Instead of having a continuous highly cross-linked extracellular protein scaffold surrounding the cells, the extracellular matrix (ECM) of the brain is composed of a relatively low content of fibrous proteins but is highly enriched in proteoglycans such as aggrecan and tenascin and glycosaminoglycans including hyaluronic acid. These components are known for their role in regulating cell proliferation, adhesion, and differentiation.[4]

It is widely documented that cells can sense and respond to the stiffness of their surroundings,[5] in a manner that depends on the cytoskeleton and the transmembrane complexes such as integrins that adhere the cell to the substrate.[6] Neurons, astrocytes, and glioma cells in culture and in tissue preparations all respond to changes in substrate mechanics.[7] Identifying the mechanosensing mechanism is important for understanding and potentially reversing the development of pathological processes in which increased stiffening is observed, including, for example, breast cancer, where stiffness alterations are so significant that the tumor can be localized by physical palpation or liver fibrosis, where stiffness is postulated to be a causative factor of liver cirrhosis.[8,9] For such diseases, a connection between increased matrix stiffness and increased cell proliferation, motility, and aggressiveness have been observed.[10,11] Interestingly, the opposite correlation was observed for metastatic ovarian cancer cells, which in vivo metastasize preferentially to soft and fatty

omentum and in laboratory settings display a more malignant phenotype on softer matrices than on stiffer ones.[12]

In this context, glioblastoma and other brain tumors are a unique category of cancer, since multiple studies of glioma stiffness have led to different results both in vitro and in vivo, suggesting that whether the mechanical properties of the tumor are altered might depend more strongly on geometry or the conditions under which the viscoelasticity is measured than for other tumor types for which a consensus is apparent. Some studies show increased stiffness in glial cell-derived tumors.[13–15] In other studies either the shear modulus of glioma tissue was softer than that of normal tissue from the contralateral side[16] or increased stiffening was not observed for the large majority of samples when studied in vivo by ultrasound elastography[17,18] or ex vivo with microindentation[19,20] unless the tissue was compressed. An important finding not generally considered in studies of tumor stiffness is that even when tumor elastic moduli are indistinguishable from those of normal tissue, there is a large difference in viscosity, with gliomas showing less viscous response than adjacent nonmalignant tissue.[17] Thus it is not evident that mechanosensing by glioblastoma cells is a universally clinically relevant modulator of cell behavior or whether another factor triggers the same responses in vivo that are produced by mechanical stimuli in vitro. To address this question the unique composition of brain ECM and the glioblastoma microenvironment has to be taken into account.

Hyaluronic acid (HA) is proposed to play a role in malignant glioma development, and its tissue content can be correlated with malignancy and poor GBM prognosis.[21] HA interacts with cells mechanically by linking through transmembrane receptors, like CD44 and RHAMM, and these linkages can regulate cell adhesion and motility. AFM-based force spectroscopy demonstrated physical binding between HA and CD44 with rupture force between 60 and 90 pN, which is similar to forces needed to unbind integrin–ligand complexes.[22,23] Hyaluronic acid is a large, linear, negatively charged macromolecule that forms viscous liquids and cross-linked 3D structures and is believed to play a structural role in brain ECM formation and function. Its role in mechanical properties of the brain is not fully understood, but in other materials like cartilage it acts to retain water and resist compression while allowing compliance in shear. Depletion of HA in pancreatic ductal carcinoma results in decreased interstitial fluid pressure.[24]

Cancer cells undergo many molecular changes that are involved in tumor growth and metastasis. These changes include altered expression of cytokines and growth factors, loss of responsiveness to cell-cycle control proteins or self-destruct signals, and many others. Among these changes, overexpression of interleukin 8 is associated with malignancy. IL-8 has a capacity to modulate the tumor microenvironment by enhancing cell proliferation and migration, by modifying communication between different cell types, by promoting preangiogenic responses in endothelial cells, and by activating tumor-associated macrophages.[25] The majority of glioblastomas exhibit an elevated concentration of IL-8 as detected both in tumor specimens and in glioblastoma cell lines grown in vitro.[26]

All of these findings represent major problems in understanding glioblastoma progression and support the hypothesis that glioblastoma cells' interaction with their environment is a

key part of their aggressive nature. In an effort to determine the extent to which altered mechanosensing can drive glioblastoma development, we performed a series of experiments using different cell lines and substrates with controlled stiffness. Taking into account GBM heterogeneity, we select three different cell lines with high metastatic potential. On the basis of our previous study,[19] we synthesized and characterized 2-D polyacrylamide and hyaluronic acid hydrogels in stiffness ranges relevant to brain and glioma mechanics. We used them to investigate the dependence of glioma cell morphology, mechanical phenotype, motility, proliferation, and IL-8 secretory potential. Our results support the hypothesis that mechanical coupling between glioblastoma cells and brain-ECM facilitates the malignant phenotype in brain but also suggest that PI3-kinase-mediated signaling from substrates containing both HA and integrin ligands can reproduce many of the phenotypes of cells on rigid substrates.

MATERIALS AND METHODS

Substrate Fabrication

Glioblastoma cells were cultured on polyacrylamide and hyaluronic acid hydrogel substrates of desired stiffness using methods previously described.[19,27] In brief, the acrylamide and bis-acrylamide solutions (BIORAD Laboratories, Hercules, CA) were prepared in double-distilled H_2O to a total volume of 1 mL. 1 μL of TEMED electrophoresis grade (Fisher BioReagents, Pittsburgh, PA) and 10 μL of 2% ammonium persulfate (Thermo Fisher Scientific, Rockford, IL) were used as polymerization initiators. Gels were polymerized between glutaraldehyde (bottom) and SurfaSil-treated (top) coverslips (Thermo Fisher Scientific). After removing the top coverslip, polyacrylamide gels were covalently linked to integrin ligands by incubating with 50 μL of 0.1 mg/mL collagen I (BD Bioscience, San Diego, CA) or 0.1 mg/mL laminin (Collaborative Biomedical, Bedford, MA) after activating the gel surface with the UV-sensitive Sulfo-SANPAH cross-linker (Thermo Fisher Scientific). Gel stiffness was adjusted to 0.31 ± 0.03, 1.04 ± 0.05, 3.50 ± 0.17, 4.54 ± 0.17, 7.99 ± 0.89, and 14.08 ± 1.28 kPa.

Native HA can be modified to induce functional groups that allow cross-linking, and resulting physicochemical properties of the hydrogels are tightly connected to the type of chemical modification applied.[28,29] In our study we used a semisynthetic HyStem Hydrogel Kit (Glycosil, BioTime) that consists of thiol-modified hyaluronan (average MW ≈ 250 kDa), thiol-reactive cross-linker PEGDA (Extralink), and sterile degassed water (DG Water). First, all of the components were allowed to come to room temperature. Then, a vial containing 10 mg of thiol-modified hyaluronan was reconstituted in 1 mL of DG water, and the vial containing 5 mg of PEGDA was reconstituted in 0.4 mL of DG water. The hyaluronan-containing vial was then placed in 37 °C for 40 min until fully dissolved, whereas PEGDA dissolved immediately. To form a hydrogel, PEGDA cross-linker was mixed in a 1:4 volume ratio with hyaluronan and supplemented with the appropriate amount of collagen I and laminin to reach a final protein concentration of 0.1 mg/mL. Gels were polymerized between the modified coverslips as for polyacrylamide hydrogels. Previous studies have shown that gels of different stiffness have the same ligand density on the surface and that there is no difference in ligand surface distribution between the gels where

protein was coated or incorporated into the gel.[27] Hyaluronic acid hydrogels stiffness was adjusted to 0.30 ± 0.03 kPa.

Hydrogel Characterization

Rheology measurements were performed using a Rheometrics RFS3 (Rheometrics, Piscataway, NJ) strain-controlled rotational rheometer fitted with 8 mm diameter parallel plates and a Peltier element incorporated in the bottom plate. For each sample, the gel solution was pipetted between the plates prior to polymerization, and the shear modulus of the polymerizing gel was measured over time by applying a constant oscillatory strain (2%) and frequency (2 rad/s). The equilibrium shear storage modulus (G'), which reflects gel stiffness, was measured after polymerization was completed. Gelation was monitored by following the kinetics of both G' and the loss modulus G'', which showed that the ratio G'/G'' as well as the magnitude of G' reached steady state 30 min after the addition of initiators. Measurements were conducted at 25 °C, and an external cover was used to prevent sample drying.

Cell Culture

Because of the strong evidence of glioblastoma tumor heterogeneity, three different glioma cell lines with distinct origin were studied. LN229 (CRL2611; ATCC, Manassas, VA) and LN18 (CRL2610; ATCC) cells were obtained from American Type Culture Collection. The LN-18 cell line was isolated from the cells of right temporal lobe of grade-IV human glioma, and the LN229 cell line was isolated from the cells taken from frontal parieto-occipital human glioblastoma. The injection of LN18 and LN229 cells into nude mice induces the formation of tumors. The LBC3 cell line was developed from human glioblastoma multiforme tissue after surgical resection, as previously described.[30] Cells were cultured in DMEM (Gibco) supplemented with 10% fetal bovine serum (FBS, Gibco, Grand Island, NY) and 100 U/mL penicillin and 100 μM streptomycin (Sigma-Aldrich, St. Louis, MO) on tissue culture plastic and kept in a humidified incubator at 37 °C and 5% CO_2.

Immunofluorescence

24 h after cell seeding, cells were fixed using 4% paraformaldehyde in PBS (Sigma-Aldrich) for 20 min and permeabilized with cold (4 °C) 0.2% Triton-X 100 solution in PBS for 5 min. For vimentin visualization, cells were incubated with primary monoclonal antibody against vimentin (1:200, Sigma-Aldrich) and antimouse Alexa Fluor 488 secondary antibody (1:500, Molecular Probes, Eugene, OR). Actin filaments and cell nuclei were visualized with rhodamine-phalloidin (1:500, Molecular Probes) and Hoechst (1:1000, Molecular Probes). Each incubation was followed by triple PBS washing, and all steps were performed at room temperature unless stated otherwise. Immunofluorescence images were recorded using a Leica DMIRE2 inverted microscope (Leica, Buffalo Grove, IL) equipped with a mercury lamp, and images were acquired using a Hamamatsu camera (Hamamatsu, Japan) and a 100× oil lens with a numerical aperture of 1.25.

Cell Area Determination

The cell adherent area was determined from optical images collected with a 40× air lens with a numerical aperture of 0.60 and phase contrast using a Hamamatsu camera on a Leica DMIRE2 inverted microscope (Leica). For each condition, a minimum of 20 images was acquired, and approximately 120–150 cells per sample were analyzed. Cell area was calculated using ImageJ software by precise tracing of single cell peripheries (ImageJ Software, NIH, Bethesda, MD). Only single cells were taken into account.

Cell Motility and Persistence Measurements

The migration speed of glioblastoma cells growing on gels and glass coverslips was determined with time-lapse microscopy over a period of 7 h in 5 min intervals. A Tokai-Hit Imaging Chamber (Tokai Hit, Shizuokaken, Japan) that maintained a humid 37 °C and 5% CO_2 environment was first equilibrated for 1 h. After 24 h of seeding, cultures were placed inside the chamber mounted on a Leica DMIRE2 inverted microscope (Leica) equipped with an ASI $x/y/z$ stage (BioVision Technologies) and a Hamamatsu camera; a 10× air lens was used for image sequence recording. Cell migration speed v (length of the total trajectory d divided by time t) was calculated by tracing the (x,y) position of the center of the cell nucleus at every image using ImageJ Software (NIH) and the Manual Tracking plugin (https://imagej.nih.gov/ij/). Total cell trajectory d can be expressed as a long discrete chain consisting of n segments of the length l ($d = n\,l$), and thus persistence length L_p was calculated using following formula

$$L_p = \frac{r^2}{n \cdot l^2} \quad (1)$$

where r (μm) is end-to-end distance (straight line that connects the first and the last points of cell trajectory) traveled by a single cell over a 7 h period, n is the number of frames taken over the 7 h period, and l is the average distance traveled by the single cell between the frames.

Results are presented as mean ± standard error of the mean (SE). Approximately 40 cells per substrate were analyzed. Cells were excluded if they migrated out of the field of view.

Cell Stiffness Measurements

Cell cortical stiffness measurements were performed using atomic force microscopy working in spectroscopy mode as previously described.[31] In brief, measurements were performed using a DAFM-2X Bioscope (Veeco, Woodbury, NY) mounted on an Axiovert microscope (Zeiss, Thornwood, NY) with silicon nitride cantilevers of a nominal spring constant of 0.06 N/m (NP-O10, Bruker, Madison, WI) and a 3.5 μm diameter polystyrene bead attached. The thermal tuning method was used for precise spring constant determination prior to the beginning of each experiment. So-called force versus distance curves were recorded on glass coverslips and successively on the sample of interest. The cantilever was moved toward the sample at the rate of 6 μm/s, and force–distance curves

were analyzed assuming Hertzian contact mechanics for a spherical indenter and Poisson ratio of the sample equal to 0.5. Cells were measured 24 h post-plating and kept in appropriate culture medium during the measurement. Approximately 100 cells per condition were analyzed.

Cell Population Doubling Time

The doubling time t_d of cells growing on different substrates was determined by plotting cell number versus time based on previously published methodology.[32] In brief, low-magnification images of the cells (10×) at 20 different locations were collected for all substrates using Leica DMIRE2 inverted microscope (Leica) every 24 h for a period of 4 days. The average cell number per field over time was fitted using an exponential growth equation: $y(t) = y_0 e^{kt}$, where y_0 is the cell number at the time point t_0, k is the growth constant, and t is time. Doubling time (t_d) was calculated using the equation $t_d = \frac{\ln 2}{k}$.[32] Results are presented as mean values and standard deviations of mean (SD).

IL-8 Expression

Media conditioned by LBC3 and LN229 cells growing on different substrates were prepared as follows. Both cell lines were seeded at a density of 40 000 cells/mL onto soft (0.3 kPa) and stiff (14 kPa) polyacrylamide and soft hyaluronic acid (0.3 kPa) hydrogels linked with collagen I or laminin or glass coverslips. 24 h post-plating, samples were transferred to new well-plates to eliminate the impact of the cells that attached to the well and not to the gel surface. 24 h later, cells were washed twice with PBS, and medium was renewed. After 24 h, conditioned media was collected into sterile eppendorf tubes and centrifuged at 1000*g* for 5 min to pellet detached and dead cells. The supernatant was collected and transferred to a new eppendorf tube. The human interleukin 8 ELISA assay (Thermo Fisher Scientific) was used for quantitative determination of IL-8 content in glioblastoma cell conditioned media according to manufacturer instructions. Simultaneously, all of the samples were imaged using a low-magnification (10× air lens) objective to estimate the total number of cells per sample. The results were normalized to the total cell number and are expressed as femtograms per cell (fg/ cell).

PI3Kinase Inhibition by Wortmannin

The effect of phosphoinositide 3-kinase (PI3Ks) inhibition on LN229 cell adherent area was quantified using time-lapse microscopy. The PI3-kinase inhibitor wortmannin was dissolved in DMSO to a concentration of 1 mM, and a working solution of 20 nM was prepared in cell culture medium (DMEM + 10% FBS) and used immediately for each experiment. LN229 cells were grown on 0.3 kPa hyaluronic acid and 14 kPa polyacrylamide gels with 0.1 mg/mL collagen I, as described above. After 24 h, cells were transferred to a live cell imaging chamber mounted on a Leica DMIRE2 inverted microscope (Leica) and observed with a 10× lens for 1 h prior to wortmannin treatment. Then, wortmannin was added to a final concentration of 20 nM and time-lapse microscopy for a period of 2 h with 30 s intervals was started. Changes of cell adherent area over time were quantified with ImageJ software by tracing single-cell peripheries (ImageJ Software, NIH). A control experiment with DMSO only was performed in parallel.

Statistical Analysis

Mean values ± standard errors of the mean (SE) are presented unless otherwise stated. Each experiment was performed at least in triplicate. The unpaired Student's *t* test with 95% confidence interval was used to confirm statistical differences between the measured quantities. Denotations: *, $P \leq 0.05$; **, $P \leq 0.01$; ***, $P \leq 0.001$; ns, $P > 0.05$, no significant differences. The two-sample Kolmogorov–Smirnov test with 95% confidence interval was used to confirm statistical differences between the distributions of cell area in Figures 2B and 7B–E. The *p* value was computed from maximum distance between the distributions of two data sets, and *p* values that are <0.05 denote that two data sets differ significantly.

RESULTS

Cell Area Is Regulated Not Only by Substrate Stiffness but Also by Its Composition

Three glioblastoma cell lines were plated on polyacrylamide hydrogels with stiffness ranging from 0.3 up 14 kPa and coated with two types of adhesive ligand, laminin, and collagen I. Quantification of adherent cell area on polyacrylamide hydrogels with different stiffness is presented in Figure 1B,C, respectively, for collagen I or laminin used as a coating. As previously reported, glioblastoma cells respond to substrate stiffness in this range, but their area and morphology depend not only on gel stiffness but also on the type of ECM ligand used for coating.[19] On polyacrylamide gels of the lowest stiffness these glioblastoma cells fail to spread and exhibit round morphology and the smallest adherent area with little actin-rich protrusions. Increasing substrate stiffness results in increased cell area and features cell-specific preferences for collagen I or laminin. On stiffness around 1 kPa, cells start to spread and produce characteristic blebs usually observed in the early stage of cell spreading. Further increase in substrate stiffness leads to the appearance of other actin-based protrusions—filopodia and lamellipodia. Importantly, as presented in Figure 1B,C, even on the gels of the highest stiffness, cell spread area does not reach the values obtained for cells on rigid glass.

Because brain ECM exhibits a very low content of fibrous proteins but a high content of glycosaminoglycans (GAGs) and proteoglycans, the next step of this study was to substitute the nonbiological and inert polyacrylamide (PAA) with one of the most abundant GAGs in the brain matrix, hyaluronic acid (HA), as the material forming the elastic gel substrate. In contrast with PAA, hyaluronan can bind to cells through specific cell-surface receptors like CD44, RHAMM, and others.[33,34] The effect of hyaluronic acid on glioblastoma cell adhesion and spreading area can be seen in Figure 2. Despite being cultured on a substrate with stiffness as low as 0.3 kPa, when hyaluronan is present in the gel, glioblastoma cells can spread, form actin-based bundles resembling stress fibers, and have a highly developed vimentin cytoskeleton, none of which were observed in cells on 0.3 kPa polyacrylamide hydrogels.

The response to hyaluronic acid is cell-line-specific, as shown in Figure 2B. The distributions of cell areas and differences in response to collagen I and laminin show a shift toward higher values when polyacrylamide is replaced by hyaluronic acid. LBC3 cells, in particular, when grown on 0.3 kPa hyaluronic acid gels with collagen I, exhibit hallmarks

typical of well-spread cells, including large cell area, polymerized actin fibers, and large nuclear area. When collagen I is replaced by an equal amount of laminin, LBC3 cells fail to spread and develop fibrous cytoskeletal filaments. This strong integrin ligand preference is less evident for LN18 and LN229, although both cell lines are sensitive to HA.

Substrate Rigidity Regulates Cortical Stiffness of Glioblastoma Cells

The effect of ECM stiffness on glioblastoma cell stiffness was evaluated by single cell force spectroscopy. Changes in substrate stiffness in a range of 0.3 to 14 kPa were sufficient to alter glioblastoma cells' cytoskeletal organization, as reflected in changes of cortical cell stiffness. Cells cultured on highly compliant substrates had low cortical stiffness and became stiffer with increased rigidity of the substrate (Figure 3A). The contribution of ECM stiffness to glioblastoma cell mechanical properties is also influenced by the type of the ligand used for cell adhesion. LBC3 cells show a strong preference for collagen-I-coated substrates and stiffen on these substrates when they are as soft as 1 kPa, even though they have a small cell area. Moreover, cell stiffness achieved at 1 kPa is comparable to the stiffness that these cells reach on glass coverslips. On the contrary, LN229 cells stiffen more when they adhere to laminin than collagen I even though they are exposed to the same substrate stiffness. LN18 cells do not exhibit a significant protein preference, as was also observed for spreading area measurements (Figure 2B).

When polyacrylamide is substituted by hyaluronic acid, cortical cell stiffness is dramatically influenced. Cortical stiffening also depends strongly on integrin-mediated protein binding and is highly cell-line-specific. LBC3 cells stiffen remarkably on 0.3 kPa HA-collagen I matrices, whereas 0.3 kPa HA-laminin does not cause such an increase. The heterogeneity of local mechanical properties of cells is reflected in width of stiffness (E) distributions seen for cells grown on 0.3 kPa HA gels with collagen I (Figure 3B). Glioblastoma cell morphological changes induced by hyaluronic acid were previously reported, while accompanying changes in cells stiffness were not investigated.[35] We therefore tested if cell adhesive area and cell stiffness are correlated. Figure 3C shows the relation between cell elastic modulus and cell area for all conditions studied. Significant differences among the three glioblastoma cell lines can be observed. In most cases an increase in spreading area is accompanied by an increase in cell stiffness. However, the link between area and stiffness is not strictly causally linked[36] and LBC3 growing on collagen-I-coated hydrogels maintains a constant high cell stiffness independent of changes in cell area.

Cell Motility and Persistence Is Differentially Influenced by Substrate Stiffness and Composition

Cell area and stiffness represent a steady-state value at a single time point. To better understand the influence of cell-ECM mechanical interactions on the dynamics of glioblastoma progression and to test whether HA-mediated signaling contributes to cell locomotion, cell migration was measured by time-lapse live-cell imaging. Migration was quantified by determining both random speed and persistence. Speed was determined over a 7 h period starting 24 h after plating. In addition to speed, one of the main aspects of cell motility that determines migration is the directionality of cell movement, often called persistence. Persistence can be understood as the ability to follow a specific direction and

often is defined as a relation of end-to-end distance traveled by cell over a certain period of time to its total distance traveled over this period. A schematic illustration of this parameter is presented in Figure 4A. In the left panel, end-to-end distance is comparable to total distance traveled ($\vec{r} \cong d$) and results in high persistence; in the right panel, total distance traveled by cell is much bigger than the end-to-end distance and results in low persistence.

LBC3 cell motility is rigidity-responsive when the cells are grown on PAA substrates, as can be seen in Figure 4B, whereas LN229 and LN18 cell migration remains relatively substrate-insensitive. Hyaluronic acid in the substrate increases LBC3 and LN18 cell speed even though substrate stiffness remains very low, but this behavior is not observed with LN229 cells. Differential response of glioblastoma cells to substrate rigidity was previously reported by Grundy et al. and supports the hypothesis of coexistence of multiple glioblastoma cell populations with different migratory potential inside the tumor.[37] Work by Kim and Kumar also shows that glioblastoma cell motility when exposed to hyaluronic acid can be influenced by both stiffness and adhesive ligand content.[38] The speed of a cell is not necessarily related to the persistence of its migration, and Figure 4B shows that both LBC and LN229 cells move faster on collagen-coated substrates than on laminin-coated substrates, but they move more persistently on laminin. Similarly, HA greatly increases the speed of LBC3 cells on both collagen and laminin, but it has no significant effect on persistence.

Cell Population Doubling Time Depends on Substrate Stiffness and Composition

Substrate stiffness has previously been shown to affect the entry of cells into the cell cycle, with stiffer substrates generally supporting more rapid cell division for fibroblast, smooth muscle, and breast epithelial cell lines.[39] In contrast, softer matrices can increase proliferation of cardiomyocytes.[40] Whether there are systematic differences in the response of normal and malignant cells to substrate stiffness has not been determined. Therefore, we studied the relation between cell proliferation and substrate stiffness and chemistry by measuring the increase in cell number using the same set of substrates for which morphology and motility were studied.

Glioblastoma cell proliferation can be stimulated by increasing substrate stiffness, as previously reported.[41] LBC3, LN229, and LN18 cells divide significantly faster on stiff polyacrylamide substrates compared with soft ones (except for the LBC3 cells grown on collagen I coated substrates) and at a rate comparable to that observed on stiff glass (Figure 5). The presence of hyaluronic acid allows all three glioma cell lines to shorten population-doubling time, although for LN229 cells this behavior depends on the type of adhesive ligand used. Our data provide evidence that glioblastoma cell proliferation not only depends on substrate stiffness but also is mediated by adhesion receptors like integrins and HA binding proteins.

Pro-Inflammatory IL-8 Secretion Is Altered by Substrate Stiffness and Composition

IL-8 expression, with its pro-inflammatory properties, is tightly regulated in normal tissues. Previous reports show that HA fragments can stimulate the expression of the cytokines IL-8 and TNF-α in primary human alveolar macrophages from patients with pulmonary fibrosis.

[42] The majority of human glioblastoma cell lines secrete significant levels of IL-8 into conditioned media, and human brain tumor specimens also contain increased amount of this cytokine. Glioblastomas are heterogeneous tumors that consist of not only glioma cells but also glia, neurons, macrophages, microglia, and others. Macrophage infiltration correlates with the histologic grade of glioblastoma, and apart from IL-8 secretion, activated macrophages can release TNF-α and IL-1, which likely have a pro-tumorigenic effect on GBM cells and facilitate their IL-8 production.[26] Massive influx of immune cells, like macrophages, can also be associated with local increase in tissue stiffness, which is a common symptom of inflammation, but does not necessarily cause the stiffening of ECM but rather increases the interstitial fluid pressure.[43] To assess if changes in substrate stiffness or the presence of hyaluronic acid as an adhesive ligand will modulate IL-8 secretion in glioblastoma cells, we tested the presence of IL-8 in media conditioned by LBC3 and LN229 cells grown on glass, soft (0.3 kPa), and stiff (14 kPa) polyacrylamide gels as well as hyaluronic acid gels with laminin or collagen I used as an adhesive ligand (Figure 6).

Our findings show that whereas the level of IL-8 secreted when cells grow on a glass coverslip is comparable for LBC3 (0.58 ± 0.15 fg/cell) and LN229 (0.50 ± 0.20 fg/cell) cells, its level detected in conditioned media collected from gel specimens differs considerably. LBC3 cells secrete more cytokine when grown on gel substrates compared with glass, and secretion is inversely correlated with gel stiffness. Moreover, the highest secretion is observed for cells grown on soft HA gels. In contrast, LN229 cells secrete less cytokine when grown on gel substrates than on glass, but again secretion depends on gel stiffness. Importantly, the presence of IL-8 in conditioned media depends strongly on type of the protein used as an adhesive ligand, which can be seen, for example, for LN229 cells when grown on hyaluronic acid gels with laminin or collagen I. This result suggests a role for outside-in integrin signaling as well as HA-dependent signaling in cytokine secretion.

Requirement for PI-3 Kinase Activity for Glioma Cell Spreading on Soft HA Gels but Not Stiff Gels with Only Integrin Ligands

Hyaluronic acid is known to modulate the PI3K/AKT signaling pathway in cancer, which leads proximally to increased levels of phosphatidylinositol trisphosphate (PIP3) and downstream to integrin activation, increased cell migration, and increased cell proliferation.[44] Wortmannin is a potent and selective inhibitor of PI3K and forms a covalent bond with lysine localized within the ATP-binding site of PI3-kinase.[45] To test whether spreading of glioblastoma cells on polyacrylamide and hyaluronic acid gels is PI3K-dependent, we treated them with 20 nM wortmannin and observed the change of cell area as a result of treatment. Within the first 10 min post-treatment, cells decreased in adherent area, as shown in Figure 7A. LN229 cells grown on a 14 kPa polyacrylamide hydrogel with collagen I started to recover their adherent area significantly after ~40 min, and this increase was continued over the rest of the measurement. Cells grown on soft hyaluronic acid gels with collagen I, despite having spread morphology before wortmannin treatment, became round and small when PI3K was inhibited and did not restore their spreading area over the time of observation, as can be seen in Figure 7A,E.

DISCUSSION

The glioblastoma cell malignant phenotype can be driven not only mechanically but also biochemically by exposing cells to brain-mimicking environments with a high content of hyaluronic acid. This activation can manifest in changes in cell spreading area, cortical stiffness, motility, proliferation, and secretion. Adhesion to collagen I or laminin triggers cell-specific responses and determines the mechanical response to substrate stiffness, which supports the importance of integrin-mediated signaling in cell-ECM adhesion in brain. This signaling can be modified when integrins and HA receptors bind simultaneously. Our findings show that glioblastoma cells respond to soft matrices with hyaluronic acid similarly to their response on stiff polyacrylamide hydrogels. Binding to hyaluronic acid can enhance the motility of glioblastoma cells in an integrin-dependent manner, as observed for the LBC3 cell line (Figure 5B). This phenomenon was previously reported in a system where soluble HA was added to cells in a membrane and was postulated to depend on activation of the PI3K/AKT pathway.[44]

The results obtained from all three cell lines show that activation of cell spreading, stiffening, motility, secretion, and in some cases proliferation can be stimulated to similar levels by either a stiff microenvironment or the presentation of integrin ligands in a soft matrix also containing cross-linked HA. Glioma cell activation by substrate stiffness has previously been reported[19,41] and is similar to that reported in studies of numerous other cell types.[46] Consistent with these results, a correlation between glioblastoma aggressiveness and the stiffness of ECM enriched in tenascin C has been reported.[47] Other studies suggest that the relevance of an in vitro mechanical response to the in vivo setting in the brain is obscured by the fact that the elastic modulus of normal brain is very low, on the order of a few hundred Pascal, and the stiffness of human glioma tissue is highly variable, with different studies concluding either stiffening or softening of the tumor when measured by elastography in vivo[13–18] and no greater than that of normal brain when measured ex vivo from biopsy sections.[19] However, the values of elastic moduli measured by macroscopic rheometry of excised specimens may not reflect the local stiffness that cells encounter in intact tissue. Previous studies have shown that pressure gradients that arise in brain tumors can produce uniaxial compression that significantly increases local stiffness,[19] and there may be microstructures such as the boundaries of blood vessels or other fibers that exert larger resistance to cell-generated forces than the average stiffness measured for the tissue as a whole. These issues leave open the possibility that mechanosensing might play a role in the growth and dissemination of gliomas, and identifying optiaml stiffness ranges that alter the phenotype of specific types of glioma cells has potential for new diagnostic and therapeutic efforts.[48]

On the contrary, diminished mechanosensing has been shown to be a feature of some cancer cells,[49] and recent studies show that although averaged over a large population cultured glioma cell lines display a strong response to the stiffness of their substrate, glioma cells with a greater malignancy display a much more blunted response to these mechanical signals.[50] Therefore, other factors, such as upregulation of hyaluronic acid in the ECM of the brain, might augment glioma cell activation either alone or in concert with changes in local mechanical environment. The role of the HA receptor CD44 in promoting migration,

proliferation, and the malignant phenotype of glioma cells supports the idea that signals initiated by ECMs enriched in HA can drive tumor growth and invasion,[38,51–53] and the roles of other HA receptors remain to be determined. The effect of HA to alter cell response to integrin ligands is not universal and has often not been reported in previous studies, consistent with previous reports that the augmentation of integrin signaling by HA is highly cell-type- and integrin-ligand-specific.[27] In addition, some cell types bind HA independently of integrin activation, and cells bound in HA matrices without integrin ligand[54] or with coupled integrin ligands[27] still respond to the matrix stiffness.

The striking similarity of the effect of HA together with integrin ligands in a soft matrix and those of the same integrin ligands in much stiffer but inert polyacrylamide substrates suggests that signaling downstream of HA might activate some of the same pathways that are activated by stiffness-dependent intracellular tension. One possibility is that ligation of collagen or some other integrin ligand to matrices composed of cross-linked HA causes them to self-assemble into fibrous structures that can change local stiffness or present epitopes otherwise seen only on stiff substrates. Local structural changes and possibly local formation of collagen oligomers on HA gels cannot absolutely be ruled out, but the equally strong effect of HA to alter response to laminin, which does not form rigid fibers (Figures 2 and 3), or to RGD peptides, which neither self-assemble nor have static structures,[27] argues against this interpretation. Alternately, the effect of HA arises from simultaneous activation of multiple signaling pathways triggered by HA and those triggered by the integrin ligand. In this context, phosphoinositide signaling, which is activated by HA receptors such as CD44,[44,51,55] is a possible link between cell activation and both intracellular tension and increased HA. PIP_3 and other polyphosphoinositides (PPIs) are potent regulators of cellular actin assembly.[56] Several cytoskeletal regulators shown to be activated by the increased tension that arises when cells are grown on stiff substrates or that respond to cortical tension are also activated by PPIs in the absence of force. These proteins include talin,[57] formins,[58,59] alpha-actinin,[60] vinculin,[60,61] *N*-WASP,[62] and ezrin, a protein immediately downstream of CD44.[63] We therefore tested the hypothesis that the ability of cells to spread and stiffen their actin-rich cortices on soft HA-containing gels depends on activation of cytoskeletal pathways that can be activated either by PPIs or by force. Indeed, inhibition of PI3K with nanomolar concentrations of wortmannin resulted in significant reduction of cell adherent area (Figure 7) which could not be restored by cells on soft HA, in contrast with the recovery observed for cells growing on stiff polyacrylamide hydrogels.

CONCLUSIONS

These studies of three distinct human glioma cell lines reveal substantial heterogeneity in response to both substrate stiffness and matrices enriched in HA but also some clear patterns. All cell types respond to both mechanical and HA-mediated stimuli, but these responses depend on the type of integrin ligand embedded in the matrix and the specific cellular phenotype that is measured. The integrin-ligand dependence is consistent with the large reported heterogeneity of integrin classes expressed by different glioma and other cancer cell types. For example, LBC3 cells, which are unusual in being derived from a collagen-I-enriched tumor, also respond more strongly to substrates containing collagen I than they do to substrates with laminin. The response of these glioma cells lines to changes

in stiffness are within the range reported for other cell types, but their response to substrates containing HA is novel. The ability of soft HA-containing substrates to elicit the same phenotypes as rigid substrates has been reported for primary cells such as cardiac myocytes and appears to reflect the response of these cells to the changing ECM during development and injury.[34] Similar responses in cancer cells might reveal the mechanisms by which malignant cells interpret or manipulate both the chemical and mechanical features of their microenvironment. The implication of the PI3-kinase pathway in the ability of soft HA substrates to mimic the effects of stiff substrates suggests that chemical messengers might duplicate the intracellular signals that act downstream of physical stimuli.

Acknowledgments

This work was supported by grants from the U.S. National Institutes of Health (GM111942, EB017753 and CA193417). K.P. has been supported by the NCN scholarship ETIUDA (project no UMO-2014/12/T/NZ1/00527).

References

1. Alves TR, Lima FRS, Kahn SA, Lobo D, Dubois LGF, Soletti R, Borges H, Neto VM. Glioblastoma cells: A heterogeneous and fatal tumor interacting with the parenchyma. Life Sci. 2011; 89(15–16): 532–539. [PubMed: 21641917]
2. Sottoriva A, Spiteri I, Piccirillo SG, Touloumis A, Collins VP, Marioni JC, Curtis C, Watts C, Tavare S. Intratumor heterogeneity in human glioblastoma reflects cancer evolutionary dynamics. Proc Natl Acad Sci U S A. 2013; 110(10):4009–14. [PubMed: 23412337]
3. Mourad PD, Farrell L, Stamps LD, Chicoine MR, Silbergeld DL. Why are systemic glioblastoma metastases rare? Systemic and cerebral growth of mouse glioblastoma. Surg Neurol. 2005; 63(6): 511–9. discussion 519. [PubMed: 15936366]
4. Novak U, Kaye AH. Extracellular matrix and the brain: components and function. J Clin Neurosci. 2000; 7(4):280–290. [PubMed: 10938601]
5. Discher DE, Janmey P, Wang YL. Tissue cells feel and respond to the stiffness of their substrate. Science. 2005; 310(5751):1139–43. [PubMed: 16293750]
6. Byfield FJ, Wen Q, Levental I, Nordstrom K, Arratia PE, Miller RT, Janmey PA. Absence of filamin A prevents cells from responding to stiffness gradients on gels coated with collagen but not fibronectin. Biophys J. 2009; 96(12):5095–102. [PubMed: 19527669]
7. Franze K, Janmey PA, Guck J. Mechanics in neuronal development and repair. Annu Rev Biomed Eng. 2013; 15:227–51. [PubMed: 23642242]
8. Mueller S, Sandrin L. Liver stiffness: a novel parameter for the diagnosis of liver disease. Hepatic Med. 2010; 2:49–67.
9. Georges PC, Hui JJ, Gombos Z, McCormick ME, Wang AY, Uemura M, Mick R, Janmey PA, Furth EE, Wells RG. Increased stiffness of the rat liver precedes matrix deposition: implications for fibrosis. American journal of physiology. Gastrointestinal and liver physiology. 2007; 293(6):G1147–54. [PubMed: 17932231]
10. Schrader J, Gordon-Walker TT, Aucott RL, van Deemter M, Quaas A, Walsh S, Benten D, Forbes SJ, Wells RG, Iredale JP. Matrix stiffness modulates proliferation, chemotherapeutic response, and dormancy in hepatocellular carcinoma cells. Hepatology. 2011; 53(4):1192–205. [PubMed: 21442631]
11. Li J, Wu Y, Schimmel N, Al-Ameen MA, Ghosh G. Breast cancer cells mechanosensing in engineered matrices: Correlation with aggressive phenotype. J Mech Behav Biomed Mater. 2016; 61:208–20. [PubMed: 26874251]
12. McGrail DJ, Kieu QM, Dawson MR. The malignancy of metastatic ovarian cancer cells is increased on soft matrices through a mechanosensitive Rho-ROCK pathway. J Cell Sci. 2014; 127(12):2621–6. [PubMed: 24741068]

13. Chauvet D, Imbault M, Capelle L, Demene C, Mossad M, Karachi C, Boch AL, Gennisson JL, Tanter M. In Vivo Measurement of Brain Tumor Elasticity Using Intraoperative Shear Wave Elastography. Ultraschall Med. 2016; 37(6):584–590. [PubMed: 25876221]
14. Niu CJ, Fisher C, Scheffler K, Wan R, Maleki H, Liu H, Sun Y, Simmons CA, Birngruber R, Lilge L. Polyacrylamide gel substrates that simulate the mechanical stiffness of normal and malignant neuronal tissues increase protoporphyin IX synthesis in glioma cells. J Biomed Opt. 2015; 20(9): 098002. [PubMed: 26405823]
15. Walter C, Crawford L, Lai M, Toonen JA, Pan Y, Sakiyama-Elbert S, Gutmann DH, Pathak A. Increased Tissue Stiffness in Tumors from Mice with Neurofibromatosis-1 Optic Glioma. Biophys J. 2017; 112(8):1535–1538. [PubMed: 28445745]
16. Feng Y, Clayton EH, Okamoto RJ, Engelbach J, Bayly PV, Garbow JR. A longitudinal magnetic resonance elastography study of murine brain tumors following radiation therapy. Phys Med Biol. 2016; 61(16):6121–6131. [PubMed: 27461395]
17. Streitberger KJ, Reiss-Zimmermann M, Freimann FB, Bayerl S, Guo J, Arlt F, Wuerfel J, Braun J, Hoffmann KT, Sack I. High-Resolution Mechanical Imaging of Glioblastoma by Multifrequency Magnetic Resonance Elastography. PLoS One. 2014; 9(10):e110588. [PubMed: 25338072]
18. Reiss-Zimmermann M, Streitberger KJ, Sack I, Braun J, Arlt F, Fritzsch D, Hoffmann KT. High Resolution Imaging of Viscoelastic Properties of Intracranial Tumours by Multi-Frequency Magnetic Resonance Elastography. Clin Neuroradiol. 2015; 25(4):371–378. [PubMed: 24916129]
19. Pogoda K, Chin L, Georges PC, Byfield FJ, Bucki R, Kim R, Weaver M, Wells RG, Marcinkiewicz C, Janmey PA. Compression stiffening of brain and its effect on mechanosensing by glioma cells. New J Phys. 2014; 16:075002.
20. Streitberger KJ, Reiss-Zimmermann M, Freimann FB, Bayerl S, Guo J, Arlt F, Wuerfel J, Braun J, Hoffmann KT, Sack I. High-resolution mechanical imaging of glioblastoma by multifrequency magnetic resonance elastography. PLoS One. 2014; 9(10):e110588. [PubMed: 25338072]
21. Delpech B, Maingonnat C, Girard N, Chauzy C, Maunoury R, Olivier A, Tayot J, Creissard P. Hyaluronan and Hyaluronectin in the Extracellular-Matrix of Human Brain-Tumor Stroma. Eur J Cancer. 1993; 29(7):1012–1017.
22. Raman PS, Alves CS, Wirtz D, Konstantopoulos K. Distinct kinetic and molecular requirements govern CD44 binding to hyaluronan versus fibrin(ogen). Biophys J. 2012; 103(3):415–23. [PubMed: 22947857]
23. Weisel JW, Shuman H, Litvinov RI. Protein-protein unbinding induced by force: single-molecule studies. Curr Opin Struct Biol. 2003; 13(2):227–35. [PubMed: 12727517]
24. Provenzano PP, Hingorani SR. Hyaluronan, fluid pressure, and stromal resistance in pancreas cancer. Br J Cancer. 2013; 108(1):1–8. [PubMed: 23299539]
25. Waugh DJ, Wilson C. The interleukin-8 pathway in cancer. Clin Cancer Res. 2008; 14(21):6735–41. [PubMed: 18980965]
26. Brat DJ, Bellail AC, Van Meir EG. The role of interleukin-8 and its receptors in gliomagenesis and tumoral angiogenesis. Neuro Oncol. 2005; 7(2):122–33. [PubMed: 15831231]
27. Chopra A, Murray ME, Byfield FJ, Mendez MG, Halleluyan R, Restle DJ, Raz-Ben Aroush D, Galie PA, Pogoda K, Bucki R, Marcinkiewicz C, Prestwich GD, Zarembinski TI, Chen CS, Pure E, Kresh JY, Janmey PA. Augmentation of integrin-mediated mechanotransduction by hyaluronic acid. Biomate-rials. 2014; 35(1):71–82.
28. Kim IL, Mauck RL, Burdick JA. Hydrogel design for cartilage tissue engineering: A case study with hyaluronic acid. Biomaterials. 2011; 32(34):8771–8782. [PubMed: 21903262]
29. Bencherif SA, Srinivasan A, Horkay F, Hollinger JO, Matyjaszewski K, Washburn NR. Influence of the degree of methacrylation on hyaluronic acid hydrogels properties. Biomaterials. 2008; 29(12):1739–49. [PubMed: 18234331]
30. Walsh EM, Kim R, Del Valle L, Weaver M, Sheffield J, Lazarovici P, Marcinkiewicz C. Importance of interaction between nerve growth factor and 91 integrin in glial tumor angiogenesis. Neuro-Oncology. 2012; 14(7):890–901. [PubMed: 22611032]
31. Pogoda K, Jaczewska J, Wiltowska-Zuber J, Klymenko O, Zuber K, Fornal M, Lekka M. Depth-sensing analysis of cytoskeleton organization based on AFM data. Eur Biophys J. 2012; 41(1):79–87. [PubMed: 22038077]

32. Maret D, Gruzglin E, Sadr MS, Siu V, Shan W, Koch AW, Seidah NG, Del Maestro RF, Colman DR. Surface expression of precursor N-cadherin promotes tumor cell invasion. Neoplasia. 2010; 12(12):1066–80. [PubMed: 21170270]
33. Turley EA, Noble PW, Bourguignon LY. Signaling properties of hyaluronan receptors. J Biol Chem. 2002; 277(7):4589–92. [PubMed: 11717317]
34. Chopra A, Lin V, McCollough A, Atzet S, Prestwich GD, Wechsler AS, Murray ME, Oake SA, Kresh JY, Janmey PA. Reprogramming cardiomyocyte mechanosensing by crosstalk between integrins and hyaluronic acid receptors. J Biomech. 2012; 45(5):824–831. [PubMed: 22196970]
35. Ananthanarayanan B, Kim Y, Kumar S. Elucidating the mechanobiology of malignant brain tumors using a brain matrix-mimetic hyaluronic acid hydrogel platform. Biomaterials. 2011; 32(31):7913–7923. [PubMed: 21820737]
36. Tee SY, Fu JP, Chen CS, Janmey PA. Cell Shape and Substrate Rigidity Both Regulate Cell Stiffness. Biophys J. 2011; 100(5):L25–L27. [PubMed: 21354386]
37. Grundy TJ, De Leon E, Griffin KR, Stringer BW, Day BW, Fabry B, Cooper-White J, O'Neill GM. Differential response of patient-derived primary glioblastoma cells to environmental stiffness. Sci Rep. 2016; 6:23353. [PubMed: 26996336]
38. Kim Y, Kumar S. CD44-Mediated Adhesion to Hyaluronic Acid Contributes to Mechanosensing and Invasive Motility. Mol Cancer Res. 2014; 12(10):1416–1429. [PubMed: 24962319]
39. Klein EA, Yin LQ, Kothapalli D, Castagnino P, Byfield FJ, Xu TN, Levental I, Hawthorne E, Janmey PA, Assoian RK. Cell-Cycle Control by Physiological Matrix Elasticity and In Vivo Tissue Stiffening. Curr Biol. 2009; 19(18):1511–1518. [PubMed: 19765988]
40. Yahalom-Ronen Y, Rajchman D, Sarig R, Geiger B, Tzahor E. Reduced matrix rigidity promotes neonatal cardiomyocyte dedifferentiation, proliferation and clonal expansion. eLife. 2015; 4:e07455.
41. Ulrich TA, de Juan Pardo EM, Kumar S. The mechanical rigidity of the extracellular matrix regulates the structure, motility, and proliferation of glioma cells. Cancer Res. 2009; 69(10):4167–74. [PubMed: 19435897]
42. McKee CM, Penno MB, Cowman M, Burdick MD, Strieter RM, Bao C, Noble PW. Hyaluronan (HA) fragments induce chemokine gene expression in alveolar macrophages - The role of HA size and CD44. J Clin Invest. 1996; 98(10):2403–2413. [PubMed: 8941660]
43. Heldin CH, Rubin K, Pietras K, Ostman A. High interstitial fluid pressure - An obstacle in cancer therapy. Nat Rev Cancer. 2004; 4(10):806–813. [PubMed: 15510161]
44. Kim MS, Park MJ, Moon EJ, Kim SJ, Lee CH, Yoo H, Shin SH, Song ES, Lee SH. Hyaluronic acid induces osteopontin via the phosphatidylinositol 3-kinase/Akt pathway to enhance the motility of human glioma cells. J Cancer Res Clin Oncol. 2006; 65(3):686–691.
45. Liu PX, Cheng HL, Roberts TM, Zhao JJ. Targeting the phosphoinositide 3-kinase pathway in cancer. Nat Rev Drug Discovery. 2009; 8(8):627–644. [PubMed: 19644473]
46. Chin LK, Xia YT, Discher DE, Janmey PA. Mechanotransduction in cancer. Curr Opin Chem Eng. 2016; 11:77–84. [PubMed: 28344926]
47. Miroshnikova YA, Mouw JK, Barnes JM, Pickup MW, Lakins JN, Kim Y, Lobo K, Persson AI, Reis GF, McKnight TR, Holland EC, Phillips JJ, Weaver VM. Tissue mechanics promote IDH1-dependent HIF1alpha-tenascin C feedback to regulate glioblastoma aggression. Nat Cell Biol. 2016; 18(12):1336–1345. [PubMed: 27820599]
48. Bangasser BL, Shamsan GA, Chan CE, Opoku KN, Tuzel E, Schlichtmann BW, Kasim JA, Fuller BJ, McCullough BR, Rosenfeld SS, Odde DJ. Shifting the optimal stiffness for cell migration. Nat Commun. 2017; 8:15313. [PubMed: 28530245]
49. Lin HH, Lin HK, Lin IH, Chiou YW, Chen HW, Liu CY, Harn HI, Chiu WT, Wang YK, Shen MR, Tang MJ. Mechanical phenotype of cancer cells: cell softening and loss of stiffness sensing. Oncotarget. 2015; 6(25):20946–58. [PubMed: 26189182]
50. Wong SY, Ulrich TA, Deleyrolle LP, MacKay JL, Lin JM, Martuscello RT, Jundi MA, Reynolds BA, Kumar S. Constitutive activation of myosin-dependent contractility sensitizes glioma tumor-initiating cells to mechanical inputs and reduces tissue invasion. Cancer Res. 2015; 75(6):1113–22. [PubMed: 25634210]

51. Sohara Y, Ishiguro N, Machida K, Kurata H, Thant AA, Senga T, Matsuda S, Kimata K, Iwata H, Hamaguchi M. Hyaluronan activates cell motility of v-Src-transformed cells via Ras-mitogen-activated protein kinase and phosphoinositide 3-kinase-Akt in a tumor-specific manner. Molecular biology of the cell. 2001; 12(6):1859–68. [PubMed: 11408591]
52. Maherally Z, Smith JR, Ghoneim MK, Dickson L, An Q, Fillmore HL, Pilkington GJ. Silencing of CD44 in Glioma Leads to Changes in Cytoskeletal Protein Expression and Cellular Biomechanical Deformation Properties as Measured by AFM Nanoindentation. Bionanoscience. 2016; 6(1):54–64.
53. Smith JR, Maherally Z, Ghoneim MK, Dickson JL, An Q, Fillmore HL, Pilkington GJ. Afm Stiffness Measurements of Glioma Cells and Cytoskeletal Protein Analysis Following Cd44 Knockdown: Implications for Glioma Cell Invasion. Neuro-Oncology. 2014; 16:vi8.
54. Shen YI, Abaci HE, Krupski Y, Weng LC, Burdick JA, Gerecht S. Hyaluronic acid hydrogel stiffness and oxygen tension affect cancer cell fate and endothelial sprouting. Biomater Sci. 2014; 2(5):655–665. [PubMed: 24748963]
55. Ghatak S, Misra S, Toole BP. Hyaluronan oligosaccharides inhibit anchorage-independent growth of tumor cells by suppressing the phosphoinositide 3-kinase/Akt cell survival pathway. J Biol Chem. 2002; 277(41):38013–20. [PubMed: 12145277]
56. Yin HL, Janmey PA. Phosphoinositide regulation of the actin cytoskeleton. Annu Rev Physiol. 2003; 65:761–789. [PubMed: 12471164]
57. Sen S, Ng WP, Kumar S. Contributions of talin-1 to glioma cell-matrix tensional homeostasis. J R Soc, Interface. 2012; 9(71):1311–7. [PubMed: 22158841]
58. Kozlov MM, Bershadsky AD. Processive capping by formin suggests a force-driven mechanism of actin polymerization. J Cell Biol. 2004; 167(6):1011–7. [PubMed: 15596547]
59. Ramalingam N, Zhao H, Breitsprecher D, Lappalainen P, Faix J, Schleicher M. Phospholipids regulate localization and activity of mDia1 formin. Eur J Cell Biol. 2010; 89(10):723–32. [PubMed: 20619927]
60. Fukami K, Endo T, Imamura M, Takenawa T. alpha-Actinin and vinculin are PIP2-binding proteins involved in signaling by tyrosine kinase. J Biol Chem. 1994; 269(2):1518–22. [PubMed: 8288618]
61. Rubashkin MG, Cassereau L, Bainer R, DuFort CC, Yui Y, Ou G, Paszek MJ, Davidson MW, Chen YY, Weaver VM. Force engages vinculin and promotes tumor progression by enhancing PI3K activation of phosphatidylinositol (3,4,5)-triphosphate. Cancer Res. 2014; 74(17):4597–611. [PubMed: 25183785]
62. Kawamura K, Takano K, Suetsugu S, Kurisu S, Yamazaki D, Miki H, Takenawa T, Endo T. N-WASP and WAVE2 acting downstream of phosphatidylinositol 3-kinase are required for myogenic cell migration induced by hepatocyte growth factor. J Biol Chem. 2004; 279(52):54862–71. [PubMed: 15496413]
63. Herrig A, Janke M, Austermann J, Gerke V, Janshoff A, Steinem C. Cooperative adsorption of ezrin on PIP2-containing membranes. Biochemistry. 2006; 45(43):13025–34. [PubMed: 17059219]

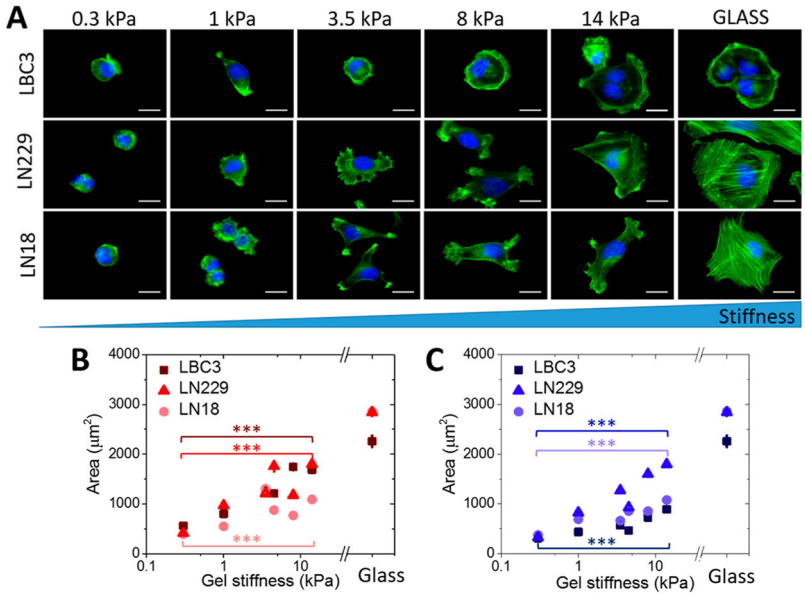

Figure 1.

Glioblastoma cell spread area as a function of substrate stiffness. (A) Fluorescent images of LBC3, LN229, and LN18 cells F-actin organization on collagen-I-coated polyacrylamide hydrogels of different stiffness (scale bar = 15 μm for all the images). (B) LBC3, LN229, and LN18 cells mean area on collagen-I-coated polyacrylamide hydrogels of different stiffness. (C) LBC3, LN229, and LN18 cells mean area on laminin-coated polyacrylamide hydrogels of different stiffness. Statistical differences were confirmed using the unpaired Student's *t* test. Horizontal lines indicate statistical significance between cells grown on 0.3 and 14 kPa PAA (denotation: ***, $P \leq 0.001$). $N \geq 100$ cells analyzed for each condition.

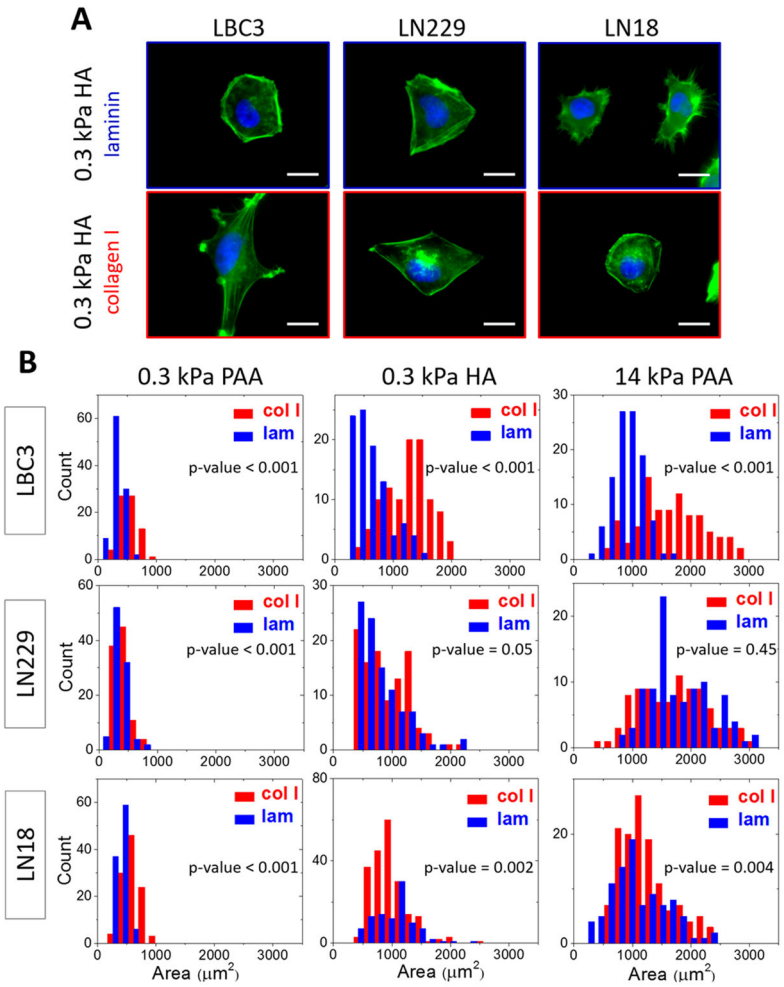

Figure 2.

Typical morphology and spreading areas of LBC3, LN229, and LN18 cell lines on different substrates. (A) LBC3 glioma cell morphology on soft (0.3 kPa) hyaluronic acid hydrogels. Cells visualized by fluorescence imaging of F-actin (green) and nucleus (blue). Scale bar = 15 μm. (B) Distributions used for quantification of cell spreading area on different substrates coated with laminin or collagen I. The two-sample Kolmogorov–Smirnov test was used to confirm statistical differences between the distributions in panel B, and associated p values are presented. $N \geq 100$ cells analyzed for each condition. Bin size is identical for all distributions and equals 175 μm^2.

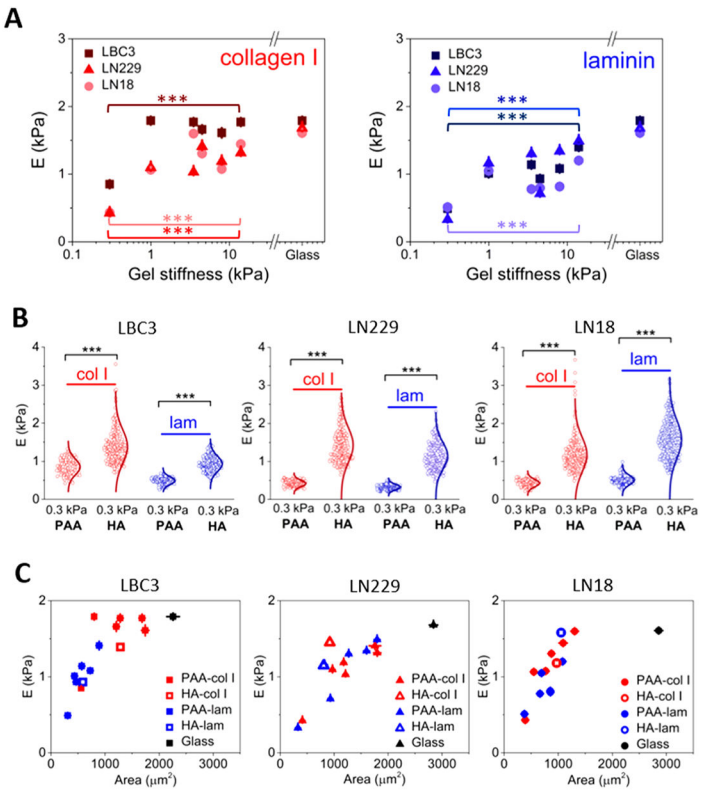

Figure 3.

Regulation of glioblastoma cell stiffness by substrate stiffness and composition. (A) Cell stiffness as a function of substrate stiffness for polyacrylamide hydrogels coated with collagen I or laminin. (B) Differences in the cell stiffness when PAA is substituted with HA. (C) Glioblastoma cell stiffness as a function of their spreading area. The unpaired Student's *t* test was used to confirm statistical differences between the cell stiffness in panels A (between 0.3 and 14 kPa PAA gels) and B (between 0.3 kPa PAA and 0.3 kPa HA); denotation: ***, $P < 0.00$).

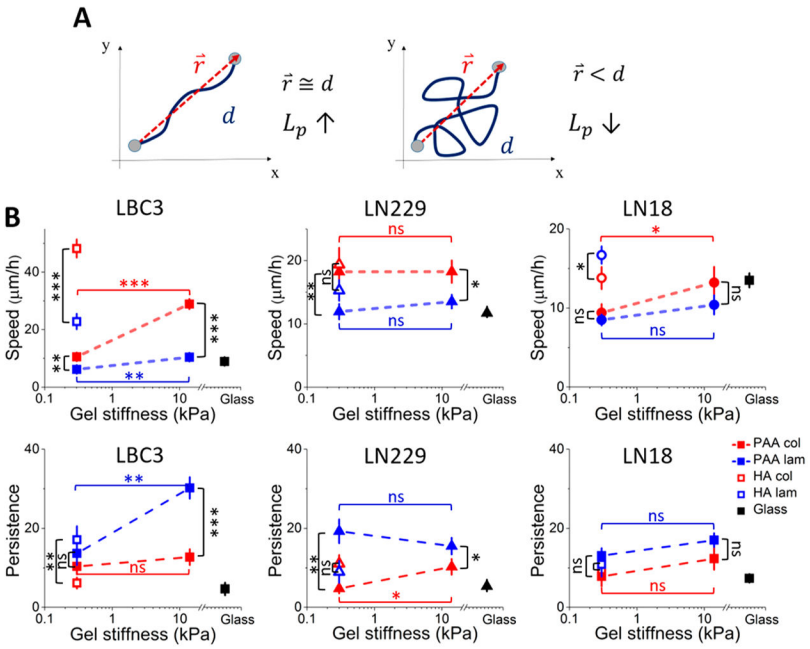

Figure 4.

Changes in cell motility as a response to substrate stiffness and composition. (A) Illustration of persistence of two different cell trajectories. (B) LBC3, LN229, and LN18 cell speed and persistence calculated based on time-lapse microscopy. Mean values ± standard deviations (SD) are presented and $N \geq 40$ cells analyzed for each condition. Statistical differences were confirmed using the unpaired Student's *t* test (denotations: *, $P \leq 0.05$; **, $P \leq 0.01$; ***, $P \leq 0.001$; ns, $P > 0.05$). Black vertical lines indicate statistical significance between PAA and HA samples of the same stiffness but with different ligand (collagen I or laminin), while horizontal red and blue lines indicate statistical significance between 0.3 and 14 kPa PAA samples with the same adhesive ligand used for coating.

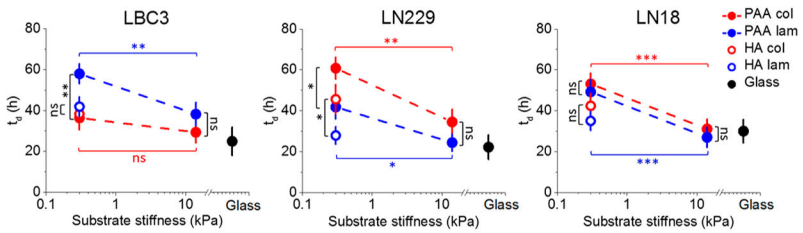

Figure 5.

LBC3, LN229, and LN18 cell population doubling time (t_d) as a function of substrate stiffness. Mean values of doubling time ± standard deviations (SD) are presented. The unpaired Student's *t* test was used to confirm statistical differences (denotations: *, $P \leq 0.05$; **, $P \leq 0.01$; ***, $P \leq 0.001$; ns, $P > 0.05$). Black vertical lines indicate statistical significance between PAA and HA samples of the same stiffness but with different ligand (collagen I or laminin), while horizontal red and blue lines indicate statistical significance between 0.3 and 14 kPa PAA samples with the same adhesive ligand used for coating.

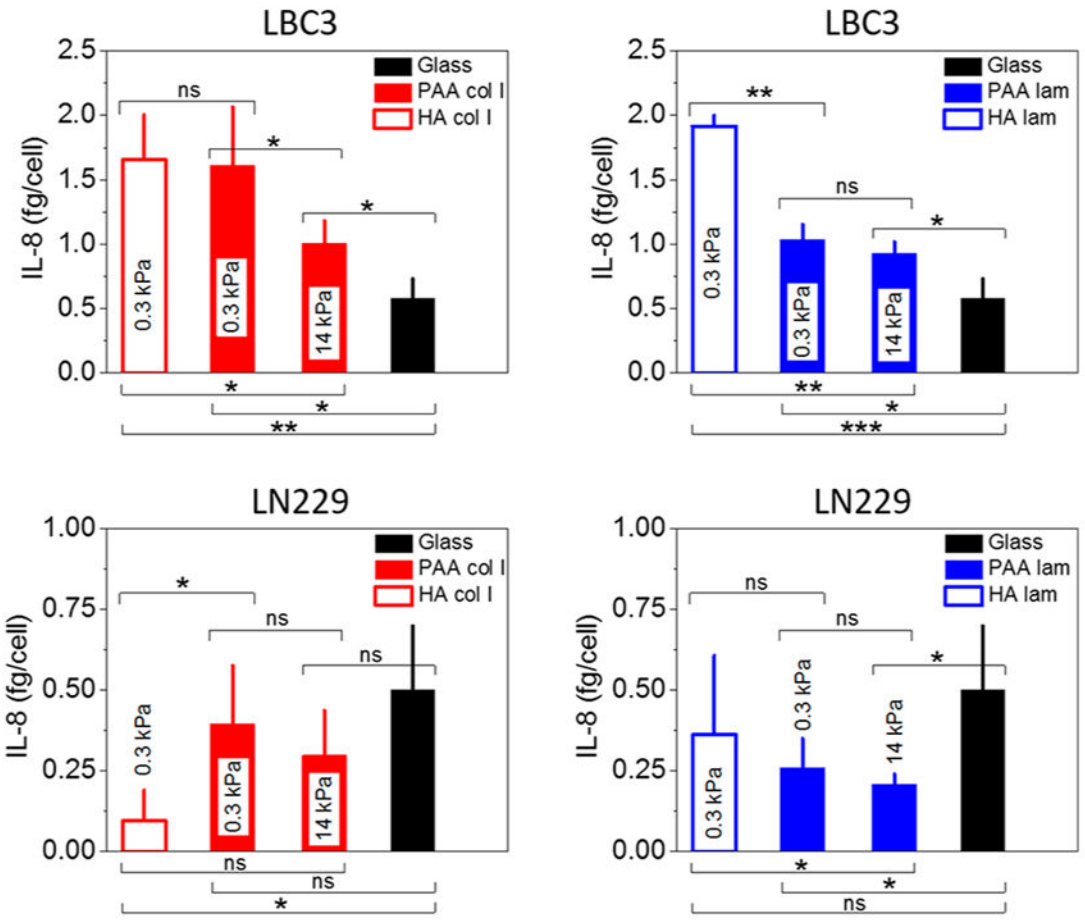

Figure 6.

IL-8 secretion by LBC3 and LN229 cells. Black columns indicate IL-8 release from cells grown on a glass surface, whereas blue and red columns indicate IL-8 release from cells grown on gels with 0.1 mg/mL laminin or collagen I, respectively. Mean values ± standard deviations (SD) are presented. The unpaired Student's *t* test was used to confirm statistical differences (denotations: *, $P \leq 0.05$; **, $P \leq 0.01$; ***, $P \leq 0.001$; ns, $P > 0.05$).

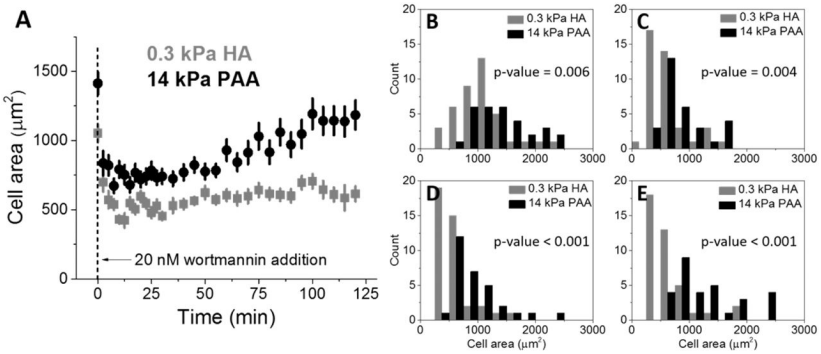

Figure 7.

LN229 cells grown on 0.3 kPa HA and 14 kPa PAA gels with collagen I and incubated with 20 nM wortmannin over the period of 2 h. (A) Average LN229 cell area as a function of time after 20 nM wortmannin treatment, obtained with time-lapse microscopy. Distributions of cell spreading area on 0.3 kPa HA and 14 kPa PAA at the moment of 20 nM wortmannin addition (B) and 12.5 (C), 60 (D), and 120 min (E) post-addition. $N \geq 30$ cells analyzed for each condition. The two-sample Kolmogorov–Smirnov test was used to confirm statistical differences between the distributions in panels B–E, and associated p values are presented.